Growth and feeding of deep-sea coral *Lophelia pertusa* from the California margin under simulated ocean acidification conditions

Carlos E. Gómez[1], Leslie Wickes[2,3], Dan Deegan[1], Peter J. Etnoyer[4] and Erik E. Cordes[1]

[1] Department of Biology, Temple University, Philadelphia, PA, United States of America
[2] JHT, Inc, Orlando, FL, United States of America
[3] Thrive Blue, LLC, Denver, CO, United States of America
[4] NOAA National Center for Coastal Ocean Science, Charleston, SC, United States of America

ABSTRACT

The global decrease in seawater pH known as ocean acidification has important ecological consequences and is an imminent threat for numerous marine organisms. Even though the deep sea is generally considered to be a stable environment, it can be dynamic and vulnerable to anthropogenic disturbances including increasing temperature, deoxygenation, ocean acidification and pollution. *Lophelia pertusa* is among the better-studied cold-water corals but was only recently documented along the US West Coast, growing in acidified conditions. In the present study, coral fragments were collected at ~300 m depth along the southern California margin and kept in recirculating tanks simulating conditions normally found in the natural environment for this species. At the collection site, waters exhibited persistently low pH and aragonite saturation states (Ω_{arag}) with average values for pH of 7.66 ± 0.01 and Ω_{arag} of 0.81 ± 0.07. In the laboratory, fragments were grown for three weeks in "favorable" pH/Ω_{arag} of 7.9/1.47 (aragonite saturated) and "unfavorable" pH/Ω_{arag} of 7.6/0.84 (aragonite undersaturated) conditions. There was a highly significant treatment effect ($P < 0.001$) with an average% net calcification for favorable conditions of $0.023 \pm 0.009\%$ d^{-1} and net dissolution of $-0.010 \pm 0.014\%$ d^{-1} for unfavorable conditions. We did not find any treatment effect on feeding rates, which suggests that corals did not depress feeding in low pH/ Ω_{arag} in an attempt to conserve energy. However, these results suggest that the suboptimal conditions for *L. pertusa* from the California margin could potentially threaten the persistence of this cold-water coral with negative consequences for the future stability of this already fragile ecosystem.

Subjects Marine Biology, Climate Change Biology, Environmental Impacts
Keywords Deep-sea, Carbonate saturation, Climate change, Ocean acidification

INTRODUCTION

Global mean values of atmospheric carbon dioxide (CO_2) have increased dramatically since pre-industrial times from 280 ppm (parts per million) to about 405 ppm in 2017. This increase in atmospheric CO_2 is unprecedented in at least the past 650 thousand years during

the last four glacial cycles (*Siegenthaler et al., 2005*). As the oceans come into equilibrium with the atmosphere, there is an alteration of carbonate chemistry with an increase in the concentration of hydrogen ions and a decrease in carbonate saturation states (Ω) (*Kleypas et al., 1999*; *Caldeira & Wickett, 2003*). The aragonite saturation horizon (ASH) is a boundary in the water column at which the carbonate saturation state is equal to 1 ($\Omega = 1$), and is found at two different depths corresponding to the different carbonate polymorphs of aragonite (Ω_{arag}) and calcite (Ω_{cal}). If the water is supersaturated ($\Omega > 1$) calcification is favored, whereas if it is undersaturated ($\Omega < 1$) dissolution is favored over calcification (*Gattuso et al., 1998*; *Langdon & Atkinson, 2005*). In a biological context, the lower the saturation state, the more energy required for calcification. Although global ocean calcium carbonate saturation states remain above 1 for most shallow portions of the ocean, models forecast a significant shoaling of the saturation horizon (ASH) by mid-century (*Orr et al., 2005*). This will have negative impacts to deep-sea ecosystems, since deep-water organisms live in habitats that already experience lower saturation states than their shallower counterparts.

Lophelia pertusa is the most well-known cold-water coral (CWC) with cosmopolitan distribution at depths normally between 40 and 800 m (*Roberts et al., 2009*). Hard substrate, local topography, temperature, current flow, and food supply have been cited as factors that can affect its distribution (*Davies & Guinotte, 2011*; *Georgian, Shedd & Cordes, 2014*). Aragonite saturation (Ω_{arag}) has also been proposed as an important factor due to the evidence that >95% of CWCs are distributed in places where the saturation of calcium carbonate is above 1 ($\Omega > 1$) (*Guinotte et al., 2006*). Nevertheless, recent deep-sea explorations have led to new observations of scleractinian corals at aragonite undersaturation, such as the Central North Pacific (*Baco et al., 2017*, ASH < 550 m), Chilean Fjords (*Fillinger & Richter, 2013*; *Jantzen et al., 2013*, ASH < 200 m), and the Central South Pacific (*Thresher et al., 2011*, ASH < 1,000 m). The mechanisms underlying this apparent ability to live under conditions that are not favorable for calcification remain unknown, since experimental studies with coral species from those places are not common. However, the capacity to alter the internal carbonate chemistry in favor of calcification has been proposed as a plausible explanation (*Raybaud et al., 2017*). Due to the significant ecological role of these deep-water habitats, understanding the complex relationship among the biology, physiology, and ecology of cold-water corals with their realized distribution is of prime importance.

The potential effects of future levels of ocean acidification on the physiological performance of CWCs have shown some contrasting evidence, nevertheless, there is good agreement about its potential negative effects (*Maier et al., 2009*; *Hennige et al., 2015*; *Georgian et al., 2016a*; *Kurman et al., 2017*). On one hand, *Form & Riebesell (2012)* studied the short and long-term response of *Lophelia pertusa* from the North Atlantic grown under different levels of pH and aragonite saturation states (Ω_{arag}). They found that in the long-term, corals were able to maintain and even increase calcification rates under high CO_2 conditions. *Büscher, Form & Riebesell (2017)* found no significant effects of low Ω_{arag} on growth rates of *L. pertusa* in the long-term, although they observed decreased calcification. On the other hand, *Kurman et al. (2017)* showed significant detrimental effects of ocean

acidification on calcification of *L. pertusa* in the long-term (6 months), and that in the short term (~2 weeks) some of the fragments experienced net dissolution rates at undersaturated levels of aragonite, although these differences were not significant due to a high variability in the response. *Georgian et al. (2016a)* found that different populations of *L. pertusa* from the Gulf of Mexico and Norwegian Skagerrak had different responses at undersaturated levels of aragonite, with the Norwegian population capable of elevating feeding rate to maintain growth at low pH, while populations of the Gulf of Mexico reduced feeding rate and calcification rates, presumably to save energy. Moreover, *Hennige et al. (2015)* showed that *L. pertusa* can survive undersaturation but with the cost of losing framework stability.

Upwelling systems are characterized by naturally higher CO_2 concentrations, and lower pH and Ω_{arag} than non-upwelling areas (*Feely et al., 2004*). These are also areas with high primary productivity, which has been shown to affect the structure and composition of the benthic fauna, including increasing deep-sea coral diversity (*Davies et al., 2008*; *Jansen et al., 2018*). The California Current System (CCS) is a key Pacific Ocean current that moves equatorward throughout the year along the west coast of North America (*Lynn & Simpson, 1987*), and is one of the four major Eastern Boundary Upwelling Systems, which has been associated with ocean acidification processes (*Feely et al., 2008*; *Gruber et al., 2012*). Modeled data have suggested that since preindustrial times, the CCS has already experienced a dramatic decrease in pH of ~0.1 and Ω_{arag} of ~0.4, with the current surface mean pH and Ω_{arag} of 7.95 ± 0.04 and 1.67 ± 0.16 respectively (*Gruber et al., 2012*). This is especially relevant given the ecological, biological, and economical importance of the CCS (*Chan et al., 2008*; *Barton et al., 2015*). In summer, when the system experiences strong upwelling, models predict undersaturation throughout the water column for coastal as well as off-shore waters (*Gruber et al., 2012*).

In order to understand the physiological response of *L. pertusa* from the California margin, we conducted a series of short-term experiments to examine the calcification and feeding behavior of corals collected from the Southern California Bight. Fragments of *L. pertusa* were grown under controlled conditions that simulated the present-day scenario *in situ* (aragonite undersaturation) hereafter referred to as "unfavorable" vs. saturated aragonite conditions (corresponding to >95% of the present-day global distribution of *L. pertusa*) hereafter referred to as "favorable". We hypothesized that corals growing in unfavorable conditions ($\Omega_{arag} < 1$) will calcify less than corals grown in favorable conditions ($\Omega_{arag} > 1$), but we still expect calcification rates to be positive (accretion > erosion). The present conditions in the California Current System are similar to those that are expected to occur by the end of the century in other areas (*Gruber et al., 2012*), so the information regarding how these corals are responding is crucial to understanding the whole ecosystem response in the CCS and beyond.

MATERIAL AND METHODS

Sample collection

Lophelia pertusa fragments were collected in the Southern California Bight (SCB) between April and May 2015 (33°55′7.6794″N; 119°28′18.84″W) at ~300 m depth under permit
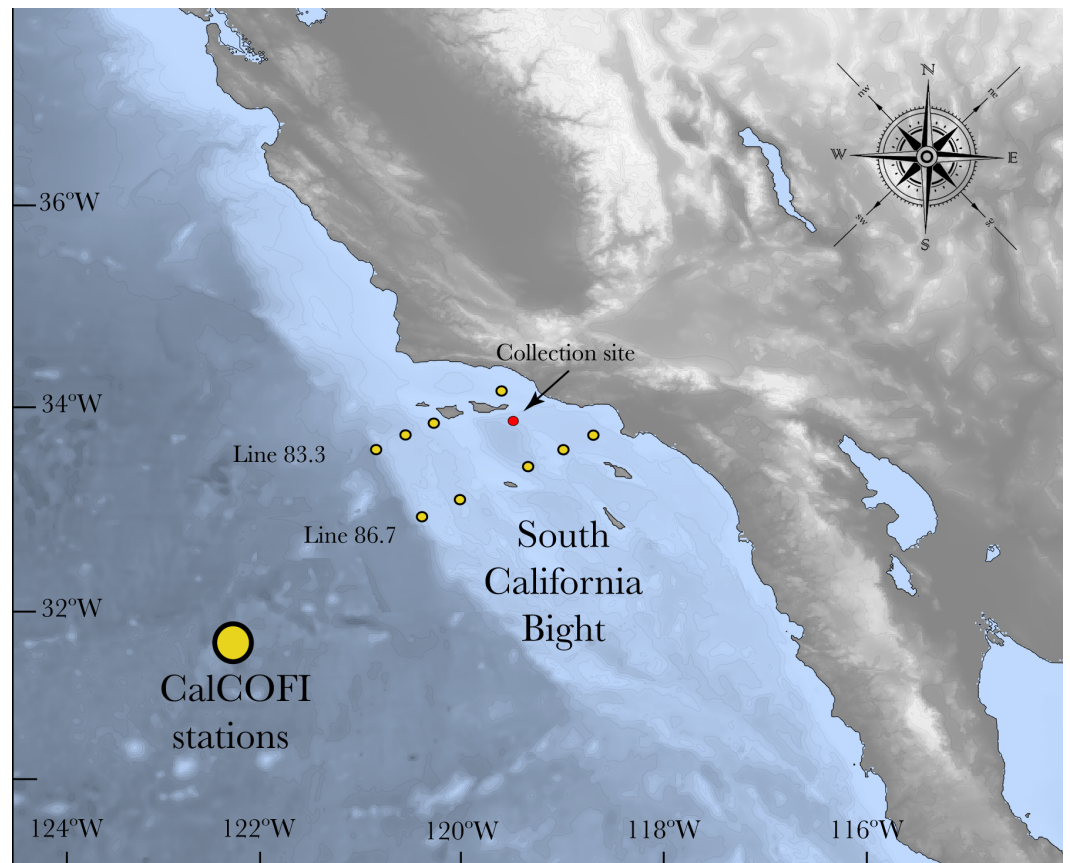
Figure 1 **Map of the South California Bight showing the sampling station (red dot).** Yellow dots refer to the CalCOFI stations used to complement the characterization of the carbonate chemistry of the area where *L. pertusa* was collected.

Full-size 🖼 DOI: 10.7717/peerj.5671/fig-1

number CINMS-2015-002, Feb 4 2015 by NOAA office of National Marine Sanctuaries in support to the project "Climate Vulnerability Assessment for Deep-Sea Corals Ecosystems in California" in order to conduct research activities in the Channel Islands National Marine Sanctuary to take resources using an ROV, and specifically to collect biological specimens (*Caldow, Etnoyer & Kracker, 2015*; Fig. 1). After collection, all live corals were kept in natural seawater at an ambient temperature of ∼9 °C using insulated containers. They were transported to the lab in Charleston, SC where they were maintained for over 1 year in a 550 L recirculating system containing custom-made artificial seawater that simulates the natural seawater conditions. Corals were maintained at a temperature of ∼9 °C , salinity 35, and total alkalinity (A_T) ∼2,300 μmol kg^{-1}. The corals were fed every other day with a mixture of zooplankton-phytoplankton (Fauna Marin®, Holzgerlingen, Germany) and artificial Marine Snow® (Two Little Fishies, Miami Gardens, FL, USA).

Seawater chemistry at the collection site

The California Current System (CCS) is an offshore water mass characterized by waters with low temperature and salinity that flow equatorward along the west coast of the US

(*Lynn & Simpson, 1987*). North Pacific Ocean water masses that influence this system are relatively low in pH and hence carbonate saturation (*Harris, DeGrandpre & Hales, 2013*; *Hauri et al., 2013*). Due to the periodic upwelling of deeper water masses, the CCS experiences frequent periods of aragonite undersaturation, which are similar to the future effects of ocean acidification in other areas (*Feely et al., 2008*; *Hauri et al., 2009*; *Gruber et al., 2012*; *Barton et al., 2015*). In order to assess the carbonate chemistry near the *L. pertusa* coral collection location, two inorganic carbon parameters (pH_T and A_T) were measured from two different sources: (1) Discrete water samples obtained from seven CTD casts (August 2014, March 2015, August 2015) and (2) CTD data from the California Cooperative Oceanic and Fisheries Investigation program (CalCOFI) stations that were sampled forming a grid within the northern part of the Southern California Bight (SCB) that includes the sample collection sites (Fig. 1). Refer to CalCOFI.org for more information about the grid and stations.

The CTD rosette was deployed in the area of major coral aggregations at the Piggy Bank and Footprint coral sites (33°55′7.32″N; 119°28′19.5594″W and 33°57′48.95″N; 119°29′22.2″W respectively) in order to characterize the carbonate system in the environment in which *L. pertusa* grows (*Caldow, Etnoyer & Kracker, 2015*). The CTD rosette was composed of Niskin bottles and a Sea-Bird CTD unit that varied according to the year of collection. In 2014, the CTD rosette was composed of four Niskin bottles with CTD Sea-Bird SBE 19+, in March 2015 it was composed of 12 Niskin bottles and a Sea-Bird SBE 9, and for August 2015 it was composed of six Niskin bottles and Sea-Bird SBE 19+. Soon after collection, water samples were transferred from the Niskin to an empty and clean Nalgene HDPE bottle (250 ml) using silicone tubing, making sure no bubbles were added to the sample and filled up to the top without headspace (*Dickson, Sabine & Christian, 2007*). Water samples were brought to room temperature and the pH_T (total scale) measurement was performed in replicate within 4 h of collection (*Dickson, Sabine & Christian, 2007*). Immediately after pH_T measurement, 50 µL of a saturated solution of mercuric chloride was added to poison the sample and prevent alterations of the carbonate chemistry by biological activity (*Dickson, Sabine & Christian, 2007*). Samples were stored in a cool and dark location until further analysis for total alkalinity (A_T) at NOAA's Center for Coastal Environmental and Biomolecular Research. The other carbonate parameters were calculated from pH_T and A_T using the software CO2calc (*Robbins et al., 2010*).

Additionally, CTD data (salinity, temperature, depth and oxygen) from CalCOFI were used to provide a more complete spatial and temporal characterization of the seawater chemistry variability of the South California Bight (SCB) for 2015, the year of collection. CalCOFI is one of the most complete, large-scale, and high-quality hydrographic sampling grids, and has been conducted since 1949 along the California Current from San Francisco to Baja California. The grid consists of a series of stations in parallel lines extending perpendicular to the coast (*Bograd, Checkley & Wooster, 2003*). Since 1964, CTD casts have been taken 3–4 times a year from the surface to a depth of 500 m (*Lynn & Simpson, 1987*). In the Southern California Bight (SCB), stations are approximately 30 km separated from each other, with a relatively high occupancy compared to other stations in the grid (*Lynn & Simpson, 1987*). Using the approximations given by *Alin et al. (2012)* specifically

Table 1 Summary of seawater carbonate chemistry conditions at Piggy Bank and experimental tanks. Seawater carbonate chemistry conditions at Piggy Bank where the samples were collected and carbonate chemistry conditions in the experimental tanks. T1 trough T3 refers to the treatment conditions. Values are given as mean ± SD. Total alkalinity (A_T), pH on total scale (pH_T), partial pressure of carbon dioxide (pCO_2), bicarbonate (HCO_3^{-2}) and carbonate (CO_3^{-}) concentrations, and aragonite saturation (Ω_{arag}).

	Piggy bank	T1	T2	T3
Depth (m)	298	–:–	–:–	–:–
Temp (°C)	8.89 ± 0.6	9.59 ± 0.41	9.55 ± 0.28	10.11 ± 0.75
A_T (μmol kg^{-1})	2,278 ± 3	2,282 ± 30	2,305 ± 66	2,184 ± 65
pH_T	7.62 ± 0.01	7.89 ± 0.04	7.62 ± 0.06	7.64 ± 0.06
pCO_2 (μatm)	1,109 ± 106	580 ± 8	1,159 ± 34	1,031 ± 32
HCO_3^{-2} (μmol kg^{-1})	2,145 ± 12	2,037 ± 27	2,168 ± 64	2,042 ± 61
CO_3^{-} (μmol kg^{-1})	54 ± 5	97 ± 2	55 ± 2	56 ± 2
Ω_{arag}	0.81 ± 0.07	1.47 ± 0.03	0.83 ± 0.03	0.85 ± 0.03

developed for the SCB from the CalCOFI data, we approximated the A_T^{es} and pH_T^{es} in a grid of approximately 100 km^2 that encompasses the area where *L. pertusa* were collected in SCB (Fig. 1). From the approximated A_T^{es} and pH^{es}, we obtained the other carbonate parameters such as [pCO_2], [HCO_3^{-}], [CO_3^{-2}] and [Ω_{arag}] using the software CO2Calc (*Robbins et al., 2010*) with the dissociation constants for boric acid and K_1 and K_2 from *Leuker, Dickson & Keeling (2000)*, KHSO$_4$ from *Dickson (1990)*, total boron from *Lee et al. (2000)* and pH on the total scale (pH_T).

CTD data from 18 points that represented 10 different stations in the grid were selected, from which A_T^{es} and pH^{es} were approximated (CalCOFI Line 86.7: stations 35–40–45–55–60 and Line 83.3: stations 40–42–51–55–60). Each station was comprised of 4 points spanning one year of sampling (November 2014–March 2015–August 2015–November 2015) that were averaged in order to get one value per station with a measure of variability. Since it is known that the shallower portions (0–80 m) are more variable (*Juranek et al., 2009*; *Alin et al., 2012*), and *L. pertusa* has not been found there, we excluded these depths and the analysis was performed from 80–400 m.

Experimental set-up and seawater chemistry manipulation

Experiments were performed between June 20th and July 29th, 2016 in a temperature-controlled cold-room (~9.5 °C) at Temple University (Table 1). To test the physiological response of *L. pertusa*, we used six (6) independent 55 L tanks where the seawater chemistry was manipulated via CO_2 additions using commercially available CO_2/pH controller system (American Marine Inc., PINPOINT pH Monitor). The system is composed of a pH controller attached independently to each tank, which is connected to a solenoid valve that automatically delivers the desired concentration of CO_2 according to a pre-set pH_T value. The pH_T meters underwent a two-point Tris-HCl and AMP-HCl calibration weekly (*Dickson, Sabine & Christian, 2007*). During the time of the experiment, a 25% water change was performed every other day to ensure good seawater conditions in the recirculating tanks. The water used in this experiment consisted of synthetic seawater (B-ionic®—ESV products) from which we were able to mimic the composition and total alkalinity of the

in situ seawater chemistry. The experimental design consisted of two different pH_T/Ω_{arag} target treatments (7.60/0.8 and 7.90/1.5), and two different total alkalinity values (2,200 and 2,300 $\mu mol\ kg^{-1}$), which match *in situ* conditions for this species in the California margin (Table 1). Total alkalinity was only manipulated within the pH_T/Ω_{arag} 7.60/0.8 treatment due to space and CO_2-system restrictions. Total alkalinity was manipulated by adjusting the proportions of the different components of the custom-made artificial seawater. Logistically, we were unable to fully replicate our experiment at the tank level, thus our experimental design consisted of two tanks per treatment, with four fragments per tank. We used two (2) tanks with favorable pH/Ω_{arag} at 2,300 $\mu mol\ kg^{-1}$ A_T, two (2) tanks with unfavorable pH/Ω_{arag} at 2,300 $\mu mol\ kg^{-1}$ A_T, and two (2) tanks with unfavorable pH/Ω_{arag} at 2,200 $\mu mol\ kg^{-1}$ A_T which approximates in situ conditions.

The pH_T of the experimental tanks was gradually brought down to the desired treatment conditions at a rate of ∼0.1 pH unit day^{-1}. Total alkalinity (A_T) was measured three times a week by acid-titration (0.1 mol L^{-1} HCl) on an open-cell potentiometric autotitrator (Mettler-Toledo DL15). The autotitrator underwent a three-point pH calibration weekly (NBS, National Bureau of Standards scale), and certified reference material (CRM) for A_T was measured weekly to ensure the accuracy of titrations (Batch 141; Dickson Labs, Seattle, WA, USA), which were always within ±1% error. Salinity was measured daily using a handheld refractometer (Vital Sine™), and temperature was recorded continually using a temperature logger (Onset HOBO Pendant®). CO2calc (*Robbins et al., 2010*) was used to calculate [pCO_2], [HCO_3^-], [CO_3^{2-}], and Ω_{arag} using pH_T, A_T, salinity and temperature as input variables with the dissociation constants for boric acid and K_1 and K_2 from *Leuker, Dickson & Keeling (2000)*, $KHSO_4$ from *Dickson (1990)*, total boron from *Lee et al. (2000)* and pH on the total scale (pH_T).

Physiological measurements
Net Calcification
Net calcification was determined with the buoyant weighing technique originally described by *Jokiel, Maragos & Franzisket (1978)*. A Denver Instruments SI-64 scale with a precision of 0.1 mg was used for this purpose. Briefly, the scale was mounted on an enclosed acrylic chamber fitted with a sliding panel that prevented air movement during weighing. By means of a tungsten wire, fragments of *L. pertusa* were weighed at the beginning and at the end of the three-week exposure, hanging under the scale and immersed in a seawater bath. Fragments were never exposed to air in any of the different measurements, and each one was weighed in triplicate to account for the variability in the measurement and the scale. Salinity and temperature of the water bath at the time of the buoyant weight were kept constant at 35 psu and 8.5 °C and were used to calculate the density of the medium in order to get the standardized dry-weight for net calcification. All fragments from each treatment were weighed when the pH reached the desired level and after 21 days. The standardized dry weight of each fragment (W_a) was calculated using the following formula:

$$Wa = W_w/(1-(D_w/SD))$$

where W_w is the measured buoyant weight, D_w is the density of the seawater during measurement and SD is the coral skeletal density (2.62 g cm^{-3}). Net calcification (N_t) of

L. pertusa was calculated as the change in weight over 3-week interval and is expressed as % d^{-1}. Net calcification was calculated by the equation:

$$N_t = 100 \times ((W_{w2} - W_{w1})/(W_{w1}(T_2 - T_1)))$$

where W_{w2} and W_{w1} are the final and initial standardized buoyant weights respectively, and T_1 and T_2 equal time 1 and time 2, respectively.

Skeletal density of coral fragments was obtained following a modified protocol proposed by *Bucher, Harriott & Roberts (1998)* in 22 coral fragments from the collection site. Briefly, fragments were initially soaked in 10% bleach for three days in order to remove living tissue. After this time, they were transferred to distilled water and left for 4 weeks to displace trapped air present in the skeletal voids. During this step, the container in which the fragments were held was tapped daily to assist bubbles removal (*Bucher, Harriott & Roberts, 1998*). At the end of period, no bubbles were observable when tapping the container. Each fragment was buoyant-weighed in distilled water, oven dried for 24 h at 60 °C and then dry-weighted using a Mettler Toledo scale model AB104-S with a precision of 0.1 mg. Skeletal density was obtained with the following formula:

$$SD = D_w/(1 - (W_w/W_a))$$

where SD = skeletal density, D_w = density of weighing medium, W_w = buoyant weight, and W_a = dry weight of coral skeleton (*Jokiel, Maragos & Franzisket, 1978*).

Feeding rates

Feeding rates were determined for each of the coral fragments as capture rate of freshly hatched *Artemia salina* nauplii (~0.5 mm in length) over 1-hour interval. Experiments were conducted in a 0.8 l circular acrylic chamber with a stir bar in the bottom (all trials were set to slow flow of about 2–3 cm s^{-1}). The chamber was placed inside a water bath that helped to maintain a constant temperature and set on top of a magnetic plate. Fragments from each tank were starved for 24 h before each experimental trial and feeding rates were assessed independently for each coral fragment (4 fragments per tank). An individual coral fragment was placed inside the acrylic chamber that was filled with seawater from the same treatment tanks and left for 30 min before starting the trial. The starting density of *A. salina* was 128 ± 3 *Artemia* l^{-1} (mean ± SD). At the end of the incubation period, the seawater from the chamber was filtered and the *A. salina* were counted under the dissecting scope. Feeding rates were standardized to number of polyps and are reported as number of prey polyp^{-1} h^{-1}.

Data analysis

The response of *Lophelia pertusa* grown under different pH/Ω_{arag} levels was obtained from the calcification and feeding rates. The effects of CO_2 were analyzed in an ANOVA model with pH/Ω_{arag} levels as fixed factor (two levels). Replicate tanks were treated as random effects nested within pH/Ω_{arag} levels in order to test for possible tank effects. Since the tank factor was not significant for both response variables ($P > 0.25$), data from replicate tanks were pooled, thus individual fragments were analyzed as replicates ($n = 8$ per treatment)

Gómez et al. (2018), *PeerJ*, DOI 10.7717/peerj.5671

8/23

Table 2 Summary table of the CalCOFI physical-chemical conditions at 300 m depth. CalCOFI ancillary stations that were used to complement the characterization of the area around *L. pertusa* collection. Values for temperature (T °C), salinity (Sal), estimated pH on total scale (pH$_T^{es}$), estimated total alkalinity (A$_T^{es}$) and aragonite saturation (Ω_{arag}) represent those found at 300 m depth (estimated values according to *Alin et al., 2012*). Line and group station refer to the CalCOFI original grid code, with the relative distance to *L. pertusa* collection. Values are given as mean ± SD.

	Group station	Latitud	Longitude	Depth range (m)	Distance to collection site (km)	T°C	Sal	pH$_T^{es}$	A$_T^{es}$	Ω_{arag}
						Physical—Chemical conditions at 300 m depth				
Line 83.3	42	34°10′N	119°30′W	80–100	27	–:–	–:–	–:–	–:–	–:–
	51	33°52′N	120°8′W	80–100	58	–:–	–:–	–:–	–:–	–:–
	55	34°44′N	120°24′W	80–400	85	8.14 ± 0.02	34.21 ± 0.006	7.66 ± 0.0004	2286 ± 0.82	0.84 ± 0.001
	60	33°34′N	120°45′W	80–400	118	7.47 ± 0.03	34.11 ± 0.002	7.68 ± 0.0002	2279 ± 0.50	0.85 ± 0.002
Line 86.7	35	33°49′N	118°37′W	80–400	76	8.77 ± 0.01	34.23 ± 0.01	7.65 ± 0.003	2282 ± 0.84	0.84 ± 0.004
	40	33°39′N	118°58′W	80–400	56	8.41 ± 0.02	34.23 ± 0.005	7.65 ± 0.0004	2285 ± 0.61	0.83 ± 0.001
	45	33°29′N	111°19′W	80–400	51	8.14 ± 0.03	34.21 ± 0.002	7.66 ± 0.0005	2285 ± 0.01	0.84 ± 0.004
	55	33°09′N	120°01′W	80–400	94	7.79 ± 0.04	34.19 ± 0.002	7.67 ± 0.0006	2286 ± 0.25	0.84 ± 0.001
	60	32°59′N	120°20′W	80–400	131	7.40 ± 0.02	34.07 ± 0.006	7.69 ± 0.0009	2277 ± 0.99	0.86 ± 0.001

(*Underwood, 1997*). Shapiro–Wilk test was used to check for normality ($P = 0.21$) and Bartlett test for homogeneity of variances ($P = 0.06$). Results were considered statistically significant at a $P < 0.05$.

RESULTS

Carbonate chemistry and coral distribution in the *in-situ* collection

L. pertusa in the Piggy Bank and Footprint areas span a range of depths between 95 m and 296 m with a mean depth of 230 ± 73 m (*Wickes, 2014*). The *in situ* carbonate chemistry obtained from the targeted CTD-casts and the values approximated from the temperature, oxygen, and salinity from the CalCOFI database revealed low pH and aragonite saturation states year-round (Fig. 2). Aragonite saturation estimated from niskin bottle water sampling ranged from ~0.6 (545 m) to ~2.5 (surface 5 m), while for the data approximated from CalCOFI values ranged from ~0.81 (400 m) to ~1.4 (80 m). Average temperature, pH and Ω_{arag} at the site of sample collection (~300 m) were 8.77 ± 0.62 °C , 7.62 ± 0.03 and 0.81 ± 0.07 respectively, while conditions close to the collection site as approximated from the CalCOFI data set were 8.06 ± 0.47 °C , 7.67 ± 0.01 and 0.81 ± 0.01 respectively (Table 2). Total alkalinity (A$_T$) ranged from 2,285 (300 m) to 2,225 (80 m). The depth of the aragonite saturation horizon near the collection sites was at approximately 120 m depth (Fig. 3).

Experimental conditions

All of the measured variables, including the seawater chemistry, were kept relatively constant through the experiment with small variations due to tank maintenance and water changes (Table 1). Physical and chemical conditions were similar to the *in situ* seawater chemistry where *L. pertusa* is distributed in the South California Bight.
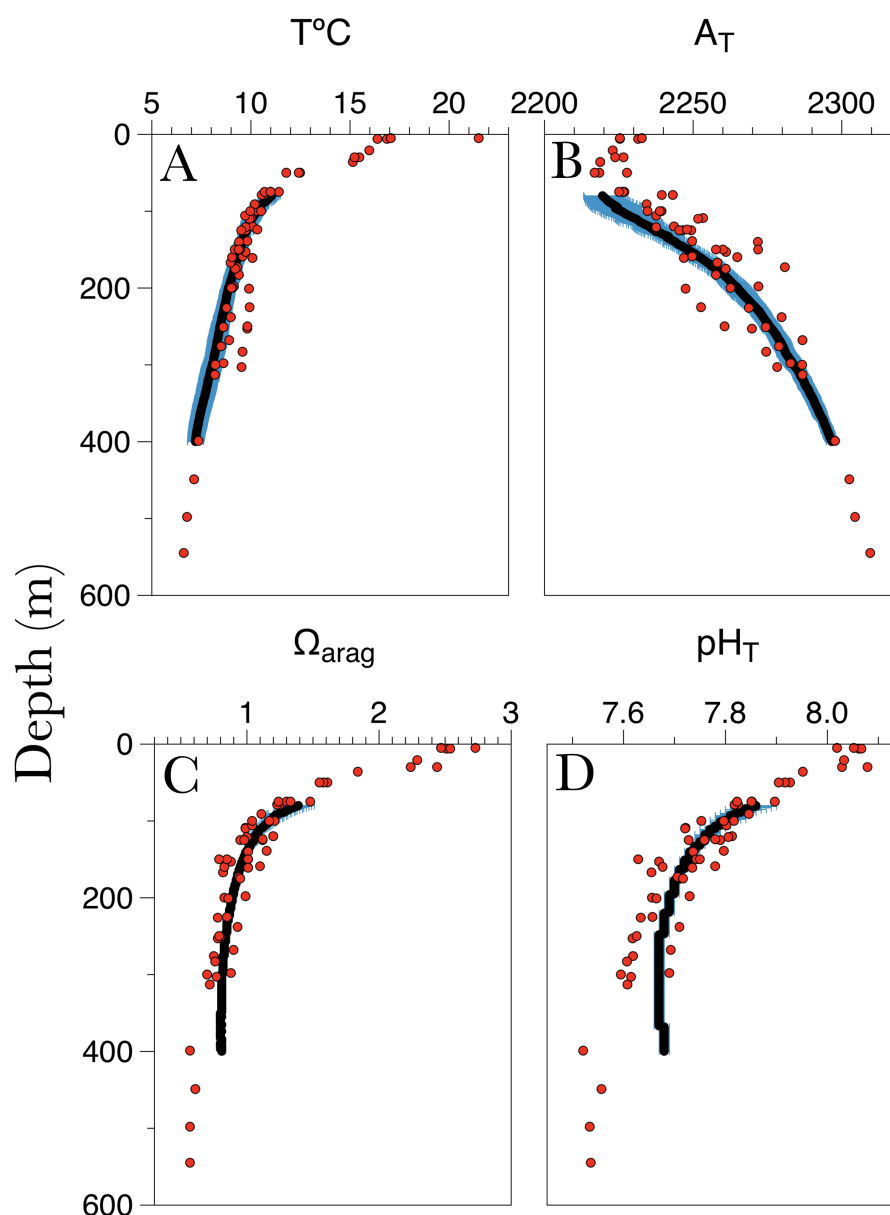
Figure 2 **Water column profiles for (A) temperature (T °C), (B) total alkalinity (A_T), (C) aragonite saturation (Ω_{arag}) and (D) pH_T (total scale) in the study site plotted against depth.** Solid line indicates the average ($\pm$SD) of the seawater chemistry approximated from the CalCOFI database spanning a whole year from Nov 2014 to Nov 2015 the red dots represent the seawater chemistry from discrete water samples taken in the area of the collection sites. pH_T^{es} and A_T^{est} where obtained from the empirical model proposed by *Alin et al. (2012)* for the South Atlantic Bight for pH_T and A_T.

Full-size ☑ DOI: 10.7717/peerj.5671/fig-2

Calcification rates

We found 100% survival of *L. pertusa* corals ($n = 24$ fragments) in the different treatments studied. The corals still appeared to be in relatively good condition, as indicated by their extended polyps. On average, corals grown in the favorable treatment ($pH_T = 7.90$,
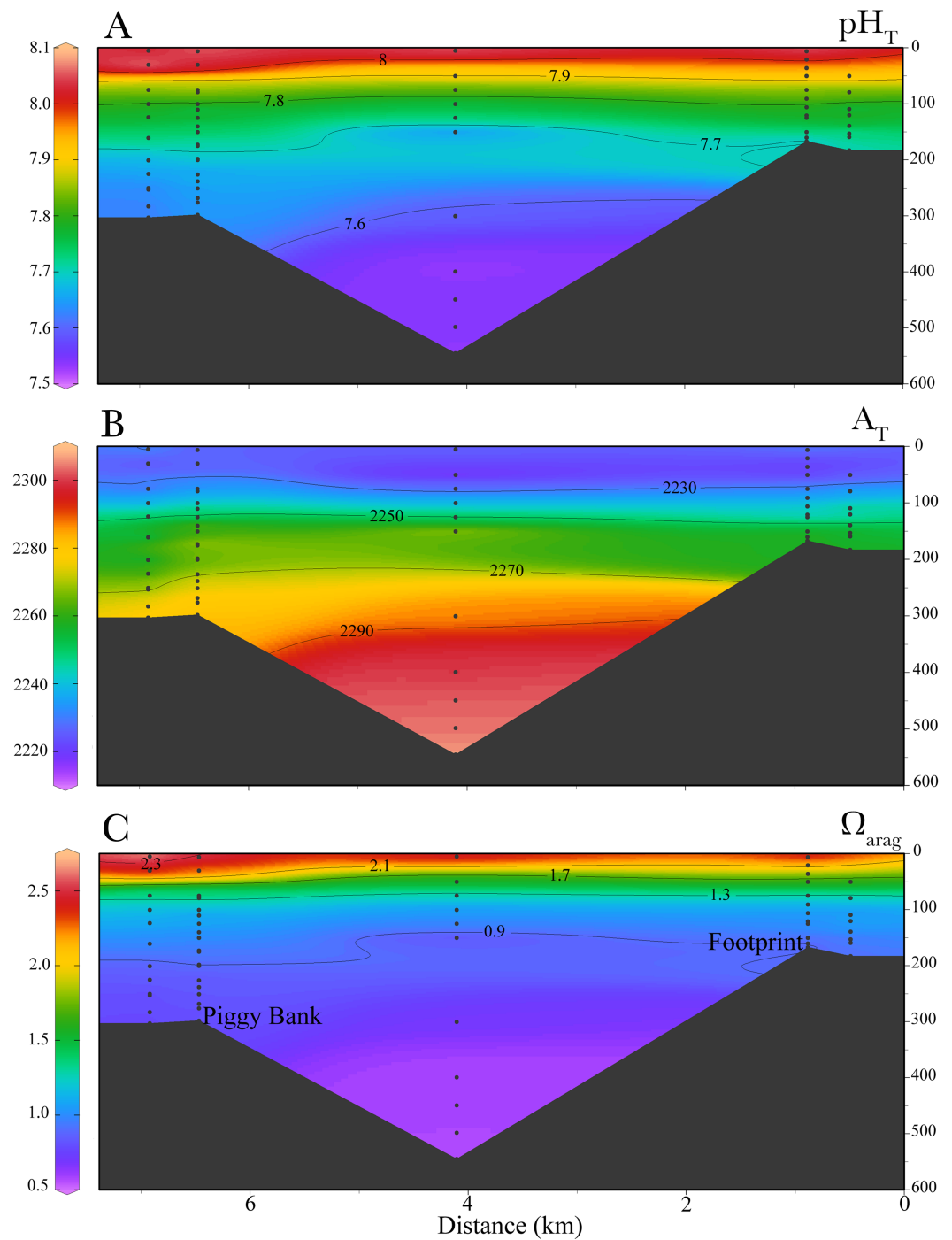
Figure 3 **Cross-sectional profiles of *in-situ* carbonate chemistry parameters.** Profiles are for (A) total pH (pH_T), (B) total alkalinity (A_T) (C) and aragonite saturation (Ω_{arag}) in the South California Bight where *L. pertusa* were collected.

Full-size ☑ DOI: 10.7717/peerj.5671/fig-3
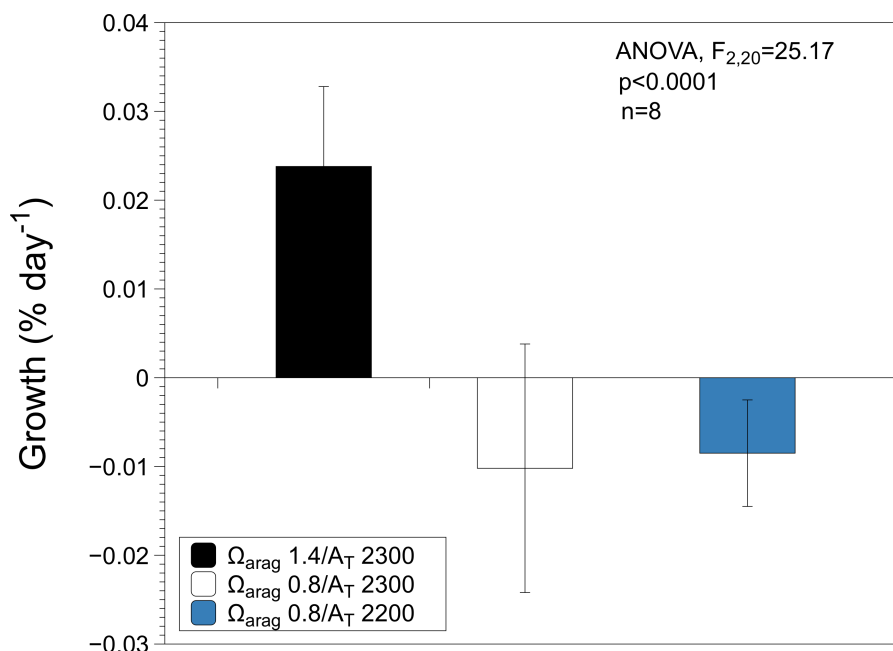
Figure 4 Growth (% day^{-1}) of *L. pertusa* fragments in the different treatment conditions. Aragonite saturation (Ω_{arag}) and total alkalinity (A_T) treatments used in the study. Values are reported as mean $\pm$ SD ($n = 8$).

$\Omega_{arag} = 1.5$) calcified at a rate of $0.02 \pm 0.009\%$ day^{-1} (mean $\pm$ SD), while for the corals grown in the unfavorable treatment (pH$_T = 7.60$, $\Omega_{arag} = 0.8$), the value was $-0.010 \pm 0.014\%$ day^{-1} (mean $\pm$ SD). Corals grown in the unfavorable treatment with low A_T calcified at a similar rate to the corals grown in the unfavorable treatment with high A_T, with net calcification rates of $-0.008 \pm 0.006\%$ day^{-1} (mean $\pm$ SD). We found a significant negative effect of pH on net calcification (ANOVA $F_{2,20} = 25.17$ $P < 0.001$) where corals grown in the unfavorable treatments experienced a decreased calcification rate with net dissolution of the skeleton by the end of the three-week period (Fig. 4, Table 3). However, there was no significant difference between A_T treatments at low pH.

Skeletal density from the 22 fragments measured were in average 2.62 ± 0.28 g cm^{-3} (mean $\pm$ SD) with a range between 1.83 and 2.83 g cm^{-3}. There was a good linear relationship between the buoyant weight and dry weight measurements taken for the calculations of the skeletal density ($R^2 = 0.98$).

Feeding rates

The average capture rate of *Artemia* in the favorable treatment were 4 ± 1 *Artemia* polyp^{-1} h^{-1} (mean $\pm$ SD) with a range of values between 2–6 *Artemia* polyp^{-1} h^{-1}. For the unfavorable treatment, the average capture rate was 3 ± 2 *Artemia* polyp^{-1} h^{-1} (mean $\pm$ SD) with a range values between 1–7 *Artemia* polyp^{-1} h^{-1}. The same pattern was observed for the capture rates in the low alkalinity treatment, which were similar to the other treatments with an average of 4 ± 4 *Artemia* polyp^{-1} h^{-1} (mean $\pm$ SD) and a range

Table 3 Summary of the response variables. Summary of the results from the response variables used to measure ocean acidification effect on fragments of *L. pertusa* in the different experimental conditions of aragonite saturation (Ω_{arag}) and total alkalinity (A_T). Values for net calcification ($G \% d^{-1}$) and feeding behavior (capture rates) are given as mean $\pm$ SD.

Treatment	N	Initial skeletal weight	Polyp #	G ($\% d^{-1}$)	Capture rates
Ω_{arag} 1.4/A_T2,300	8	9.69 $\pm$ 2.42	11 $\pm$ 4	0.0238 $\pm$ 0.009	4.09 $\pm$ 1.41
Ω_{arag} 0.8/A_T 2,300	8	11.56 $\pm$ 3.60	10 $\pm$ 5	-0.0102 ± 0.014	2.65 $\pm$ 1.99
Ω_{arag} 0.8/A_T 2,200	7	10.95 $\pm$ 4.24	9 $\pm$ 5	-0.0085 ± 0.006	3.86 $\pm$ 4.36
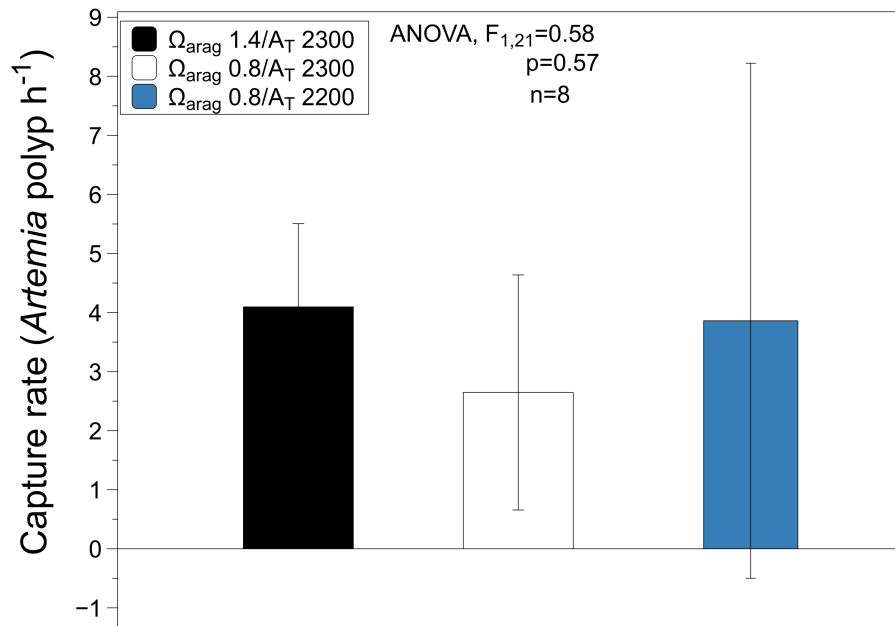
Figure 5 Average capture rates of *Artemia* standardize per polyp per hour. Aragonite saturation (Ω_{arag}) and total alkalinity (A_T) treatments used in the study. Values are reported as mean $\pm$ SD ($n = 8$).
Full-size 🖼 DOI: 10.7717/peerj.5671/fig-5

value between 1 and 14 *Artemia* polyp^{-1} h^{-1} (Fig. 5, Table 3). There were no significant differences for the capture rate of *Artemia* between treatments (ANOVA $F_{2,21} = 0.58$, $P = 0.57$).

DISCUSSION

This study shows that populations of *L. pertusa* from the South California Bight (SCB) are already experiencing negative effects of low pH and Ω_{arag}. These suboptimal conditions result in a decrease in net calcification rates in the laboratory. These experiments were carried out under the conditions it normally experiences year-round, compared to the typical conditions in other parts of its range. Calcification rates found in the present study for favorable conditions are in accordance with those found in other studies performed with *L. pertusa* under similar conditions (pH 7.9, Ω_{arag} 1.3, A_T ~2,300) (*Maier et al., 2009*; *Hennige et al., 2014*; *Lunden et al., 2014*; *Georgian et al., 2016a*). However, the negative

net calcification of −0.0102 and −0.008 G (% d^{-1}) for the low pH/ Ω_{arag} treatments are unexpected. Given the conditions in which this species grows in the SCB (pH ∼7.6 and Ω_{arag} ∼0.8), we expected positive calcification rates of coral fragments grown in the unfavorable treatment. Negative net calcification rates have been also found for *L. pertusa* from the Gulf of Mexico under similar experimental conditions (*Lunden et al., 2014*; *Georgian et al., 2016a*; *Kurman et al., 2017*), however these populations live in Ω_{arag} >1 and do not experience undersaturation yet (*Georgian et al., 2016b*). It has been documented that *L. pertusa* populations from the North Atlantic seems to be more resistant to OA effects, at least in the near future where the Ω_{arag} levels fall near the saturation horizon or slightly undersaturated (*Form & Riebesell, 2012*; *Büscher, Form & Riebesell, 2017*). We found that 100% of the coral fragments exhibited a net loss of skeleton in the acidified treatment, rendering an important concern of the fate of these scleractinians and the communities they support on the California Margin.

The findings of this study are in broad agreement with other investigations of the effects of ocean acidification on *L. pertusa*, although a wide variety of responses have been shown. *Kurman et al. (2017)* found a negative response for coral fragments from the Gulf of Mexico at the end of a 6-month period under saturation states of 0.8, and by the end of the experiment, 100% of the coral fragments showed negative calcification. However, some genotypes in this study were capable of maintaining positive net calcification significantly longer than others. In a short-term experiment using corals from these same populations, *Lunden et al. (2014)* found different responses among genotypes, with a change in the overall response around a pH of 7.75, corresponding to a saturation state of almost exactly 1. The majority of studies that have found no effect in decreasing aragonite/pH have used levels only slightly undersaturated (∼1) or still above saturation (>1) (*Maier et al., 2012*; *Movilla et al., 2014*; *Büscher, Form & Riebesell, 2017*). *Maier et al. (2016)* found negative calcification rates for *Madrepora oculata* only when the Ω_{arag} fell below a threshold of 0.9. Therefore, it is likely that the negative effects on cold-water corals are only evident when Ω_{arag} falls well below a certain threshold, and the erosive forces outweigh the accretionary forces and the calcification rate of *L. pertusa* colonies cannot keep up with the increasing rate of skeletal dissolution.

The absence of reef-framework and low proportion of live coral in the SCB has been attributed to the low saturation states of the region (*Wickes, 2014*). However, it is known that CWCs exert a strong biological control on calcification rates, elevating and or modifying the carbonate chemistry in the compartments were the calcification occurs, suggesting that CWCs are still able to produce calcium carbonate at low pH/ Ω_{arag} (*McCulloch et al., 2012*; *Raybaud et al., 2017*). *Raybaud et al. (2017)* provided a numerical framework of internal carbonate chemistry in several species of scleractinian corals, and they found that CWCs exert the strongest control on Ω_{arag}, elevating carbonate concentrations up to 10 times that of the surrounding seawater. The finding here of an independence of calcification rate on total alkalinity in the unfavorable treatment suggests that the control of Ω_{arag} is by factors other than negative ion transport, such as proton pumps controlling internal pH.

Due to the demonstrated ability of CWCs to calcify at reduced Ω_{arag}, it may be that dissolution rates are the most important variable to take into consideration when

determining overall net calcification for *L. pertusa* living at undersaturation. This rate will primarily be a function of the Ω_{arag} but also the relative degree of tissue coverage of the skeleton (i.e., *Gammon et al., 2018*). Where there is more exposed skeleton, there will be higher dissolution. This could partially explain the lower skeletal density that was measured in the corals from this study (2.62 g cm^{-3}) as compared to the corals in the Gulf of Mexico (2.81 g cm^{-3}, *Lunden, Georgian & Cordes, 2013*). Gross calcification and tissue coverage were not monitored in the present study, and therefore it is difficult to conclude whether the pattern observed is due to higher dissolution rates alone or if there is also a decline in the gross calcification rate.

In this study, feeding performance (capture rate) was similar between treatments, suggesting that pH/Ω_{arag} did not compromise the ability of a given coral nubbin to obtain food. These results contrast with other studies where *L. pertusa* can either increase feeding and respiration rates to meet the elevated energetic challenges of low pH and Ω_{arag}, or decrease feeding and respiration to undergo metabolic depression to presumably wait for a return to favorable conditions (*Houlbrèque et al., 2015*; *Georgian et al., 2016a*). Our results of prey capture (3–4 *Artemia* polyp^{-1} h^{-1}) fall within the lower range for some studies, i.e., *Lophelia pertusa* from the North Atlantic (*Purser et al., 2010*: 6 $\pm$ 1 *Artemia* polyp^{-1} h^{-1}; *Orejas et al., 2016*: 22 $\pm$ 8 *Artemia* polyp^{-1} h^{-1}; *Georgian et al., 2016a*: 8 $\pm$ 1 *Artemia* polyp^{-1} h^{-1}) and within the higher range for populations from the Gulf of Mexico (*Georgian et al., 2016a*: 2 $\pm$ 1 *Artemia* polyp^{-1} h^{-1}). The higher values normally found for the North Atlantic populations are related to the apparent higher metabolic rates in those populations (*Purser et al., 2010*; *Orejas et al., 2016*).

Food availability and nutrient supply are known to be important in shallow-water tropical systems, where additional inputs generate the extra energy required for calcification under ocean acidification (*Cohen & Holcomb, 2009*; *Houlbrèque et al., 2015*). On the other hand, some studies performed in CWCs have found that, in general, corals grown under higher food concentrations do not increase calcification rates as compared to low food concentrations (*Maier et al., 2016*; *Büscher, Form & Riebesell, 2017*), even though deep-water corals are heterotrophic organisms that rely entirely on external food supplies. Still, it is plausible that the high productivity of the California Current System, along with *L. pertusa'* s relatively shallow distribution in the area can explain why this coral population persists under the low pH and saturation state that it experiences there, although at the expense of skeletal density and framework stability. However, it is not known if these coral populations are actively growing at this time or are relics of populations that existed before the onset of ocean acidification, since the industrial revolution in the 19 century. It is important to point out that while experimental conditions in controlled systems are set-up to mimic the natural environment as close as possible, it is specially challenging to recreate the full spectrum of conditions, especially the variable food supply and nutrient availability typical of the bathyal environment.

L. pertusa is normally associated with high-energy environments, due to enhanced food supply from the surface via advection, and resuspension from internal waves and currents (*Davies et al., 2009*; *Roberts et al., 2009*). It has been shown that high surface primary productivity together with the bentho-pelagic coupling affects the structure of

the benthic fauna, including increasing deep-sea coral diversity (*Davies et al., 2008*; *Jansen et al., 2018*). *Jansen et al. (2018)* found a positive correlation between the abundance of deep-water suspension feeders (coral and sponges) and high surface primary productivity, which ultimately sinks and provides an important source of particulate organic carbon (POC). Similar patterns have been found in the North Atlantic (*Lacharité & Metaxas, 2017*) and in the Tasmanian seamounts where the abundance of the scleractinians *Solenosmilia variabilis* and *Enallopsammia rostrata* between 750–1,400 m, with peak distribution at or slightly below the ASH, can be explained by the high input of marine snow and particulate organic matter in this area (*Thresher et al., 2011*). Similarly, these species have been found in comparable conditions in the North Central Pacific, also associated with areas of high input of nutrients and productivity at the surface (*Baco et al., 2017*). Coral calcification is energetically costly and can consume up to 20% of the coral's energy budget (*Cohen & Holcomb, 2009*). This requirement can increase by 20–30% under ocean acidification scenarios expected by the end of the century (*McCulloch et al., 2012*).

In addition to ocean acidification, climate and ocean change are expected to alter primary productivity in coastal regions, as well as the rate of export to deep waters. Increasing stratification due to the more rapid rise of temperature in surface waters will reduce the export of POC to depth and the delivery of deep-water nutrients to the surface (*Palacios et al., 2004*). However, there is some evidence that increased shore wind velocity can lead to increased nutrient delivery in upwelling systems (*Bakun et al., 2015*; *Wang et al., 2015*), which if coupled with an efficient feeding behavior, CWCs from California margin might be able to increase their energy intake for metabolic function in order to keep the homeostatic control. Nevertheless, this increase in nutrients in the CCS might be counteracted by the decrease in oxygen concentration (-18%) and pH (-0.5 units) projected for this area by the end of the century (*Rykaczewski & Dunne, 2010*). *Lophelia pertusa* colonies cannot survive under low oxygen conditions based on lab experiments, although the exact limit of their tolerance appears to vary by population (<3.4 ml l^{-1}, *Dodds et al., 2007*; <1.5 ml l^{-1}, *Lunden et al., 2014*). However, further multi-stressor experiments are necessary to determine how all of these factors interact and affect *L. pertusa*. But it is clear that the outcome for specific populations is a combination of their genetic variability along with their history of food availability and therefore energetic reserves, which will result in different physiological responses to the exacerbated challenges that deep-water corals will face in the future.

CONCLUSIONS

These results highlight that *L. pertusa* is persisting along the California margin under more extreme carbonate chemistry conditions than have been found in other populations. Although our results show decreased net calcification under unfavorable Ω_{arag}, it is important to bear in mind that experimental conditions are normally tightly controlled, which does not account for the dynamics normally seen in natural conditions, especially in places with high productivity such as the California Current System. It is possible that the CCS provides an exception where an active growing population can be maintained at

undersaturated conditions of calcium carbonate as a result of elevated food availability from surface layers. *L. pertusa* is an important habitat structuring species, forming habitat for many species, including some of commercial importance, in one of the most productive regions in the world (*Barton et al., 2015*). Consequently, the ecological impacts of ocean acidification on the deep-water corals of the California Current system are of significant concern given that this region will experience year-round undersaturation most of the water column within the next 20–30 years and by 2050.

ACKNOWLEDGEMENTS

ADDITIONAL INFORMATION AND DECLARATIONS

Funding

Grant Disclosures

Competing Interests

Erik Cordes is an Academic Editor for PeerJ. Leslie Wickes was employed by JHT, Inc. at the time of the sample collection, and now is the owner and sole operator of Thrive Blue LLC.

Author Contributions

- Carlos E. Gómez conceived and designed the experiments, performed the experiments, analyzed the data, prepared figures and/or tables, authored or reviewed drafts of the paper, approved the final draft.
- Leslie Wickes conceived and designed the experiments, performed the experiments, authored or reviewed drafts of the paper, approved the final draft, in-situ carbonate chemistry analysis.
- Dan Deegan performed the experiments, authored or reviewed drafts of the paper, approved the final draft.
- Peter J. Etnoyer and Erik E. Cordes conceived and designed the experiments, contributed reagents/materials/analysis tools, authored or reviewed drafts of the paper, approved the final draft.

Field Study Permissions

The following information was supplied relating to field study approvals (i.e., approving body and any reference numbers):

Research was conducted under permit CINMS-2015-002 issued Feb 4, 2015 by NOAA Office of National Marine Sanctuaries, in support of the project "Climate Vulnerability Assessment for Deep-Sea Coral Ecosystems in California".

Data Availability

The following information was supplied regarding data availability:

The raw data are provided in the Supplemental Files.

Supplemental Information

Supplemental information for this article can be found online at http://dx.doi.org/10.7717/peerj.5671#supplemental-information.

REFERENCES

Alin SR, Feely RA, Dickson AG, Hernández-Ayón JM, Juranek LW, Ohman MD, Goericke R. 2012. Robust empirical relationships for estimating the carbonate system in the southern California Current System and application to CalCOFI hydrographic cruise data (2005–2011). *Journal of Geophysical Research Ocean* **117**:C05033 DOI 10.1029/2011JC007511.

Baco AR, Morgan N, Roark EB, Silva M, Shamberger KEF, Miller K. 2017. Defying dissolution: discovery of deep-sea scleractinian coral reefs in the North Pacific. *Scientific Reports* **7**:1–11 DOI 10.1038/s41598-017-05492-w.

Bakun A, Black BA, Bograd SJ, García-Reyes M, Miller AJ, Rykaczewski RR, Sydeman WJ. 2015. Anticipated effects of climate change on coastal upwelling ecosystems. *Current Climate Change Reports* **1**:85–93 DOI 10.1007/s40641-015-0008-4.

Barton A, Waldbusser GG, Feely RA, Weisberg SB, Newton JA, Hales B, Cudd B, Eudeline B, Langdon CJ, Jefferds I, King T, Suhrbier A, McLaughlin K. 2015. Impacts of coastal acidification on the Pacific Northwest shellfish industry and

adaptation strategies implemented in response. *Oceanography* **28**:146–159 DOI 10.5670/oceanog.2015.38.

Bograd SJ, Checkley DA, Wooster WS. 2003. CalCOFI: a half century of physical, chemical, and biological research in the California current system. *Deep-Sea Research, Part II (Topical Studies in Oceanography)* **50**:2349–2353 DOI 10.1016/S0967-0645(03)00122-X.

Bucher DJ, Harriott VJ, Roberts LG. 1998. Skeletal micro-density, porosity and bulk density of acroporid corals. *Journal of Experimental Marine Biology and Ecology* **228**:117–136 DOI 10.1016/S0022-0981(98)00020-3.

Büscher JV, Form AU, Riebesell U. 2017. Interactive effects of ocean acidification and warming on growth, fitness and survival of the cold-water coral *Lophelia pertusa* under different food availabilities. *Frontiers in Marine Science* **4**:101 DOI 10.3389/fmars.2017.00101.

Caldeira K, Wickett ME. 2003. Anthropogenic carbon and ocean pH. *Nature* **425**:365.

Caldow C, Etnoyer PJ, Kracker L. 2015. Cruise report for 'Patterns in Deep-Sea Corals' expedition: NOAA ship Bell M. Shimada SH-15-03. NOAA Technical Memorandum NOS NCCOS 200. Silver Spring, MD, 15 pp DOI 10.25923/krv2-ps85.

Chan F, Barth JA, Lubchenco J, Kirincich A, Weeks H, Peterson WT, Menge BA. 2008. Emergence of anoxia in the California current large marine ecosystem. *Science* **319**:920 DOI 10.1126/science.1149016.

Cohen AL, Holcomb M. 2009. Why corals care about ocean acidification: uncovering the mechanism. *Oceanography* **22**:118–127 DOI 10.5670/oceanog.2009.102.

Davies AJ, Duineveld GC, Lavaleye MS, Bergman MJN, Van Haren H, Roberts JM. 2009. Downwelling and deep-water bottom currents as food supply mechanisms to the cold-water coral *Lophelia pertusa* (Scleractinia) at the Mingulay Reef complex. **54**:620–629 DOI 10.4319/lo.2009.54.2.0620.

Davies AJ, Guinotte JM. 2011. Global habitat suitability for framework-forming cold-water corals. *PLOS ONE* **6(4)**:e18483 DOI 10.1371/journal.pone.0018483.

Davies AJ, Wisshak M, Orr JC, Murray Roberts J. 2008. Predicting suitable habitat for the cold-water coral *Lophelia pertusa* (Scleractinia). *Deep-Sea Research, Part I (Oceanographic Research Papers)* **55**:1048–1062 DOI 10.1016/j.dsr.2008.04.010.

Dickson AG. 1990. Standard potential of the reaction: $AgCl(s) + 1/2H_2(g) = Ag(s) + HCl(aq)$, and the standard acidity constant of the ion HSO_4^- in synthetic sea water from 273.15 to 318.15 K. *Journal of Chemical Thermodynamics* **22**:113–127 DOI 10.1016/0021-9614(90)90074-Z.

Dickson AG, Sabine CL, Christian JR. 2007. Guide to best practices for ocean CO_2 measurement. *PICES Special Publication 3*. Sidney: North Pacific Marine Science Organization, 191.

Dodds L, Roberts JM, Taylor AC, Marubini F. 2007. Metabolic tolerance of the cold-water coral *Lophelia pertusa* (Scleractinia) to temperature and dissolved oxygen change. *Journal of Experimental Marine Biology and Ecology* **349**:205–214 DOI 10.1016/j.jembe.2007.05.013.

Feely RA, Sabine CL, Hernandez-Ayon JM, Lanson D, Hales B. 2008. Evidence for upwelling of corrosive "acidified" water onto the continental shelf. *Science* **320**:1490–1492 DOI 10.1126/science.1155676.

Feely RA, Sabine CL, Lee K, Berelson W, Kleypas J, Fabry VJ, Millero FJ. 2004. Impact of anthropogenic CO_2 on the $CaCO_3$ system in the oceans. *Science* **305**:362–366 DOI 10.1126/science.1097329.

Fillinger L, Richter C. 2013. Vertical and horizontal distribution of *Desmophyllum dianthus* in Comau Fjord, Chile: a cold-water coral thriving at low pH. *PeerJ* **1**:e194 DOI 10.7717/peerj.194.

Form AU, Riebesell U. 2012. Acclimation to ocean acidification during long-term CO_2 exposure in the cold-water coral *Lophelia pertusa*. *Global Change Biology* **18**:843–853 DOI 10.1111/j.1365-2486.2011.02583.x.

Gammon MJ, Tracey DM, Marriot PM, Cummings VJ, Davy SK. 2018. The physiological response of the deep-sea coral *Solenosmilia variabilis* to ocean acidification. *PeerJ* **6**:e5236 DOI 10.7717/peerj.5236.

Gattuso JP, Frankignoulle M, Bourge I, Romaine S, Buddemeier RW. 1998. Effect of calcium carbonate saturation of seawater on coral calcification. *Global and Planetary Change* **18**:37–46 DOI 10.1016/S0921-8181(98)00035-6.

Georgian SE, Deleo D, Durkin A, Gómez CE, Kurman M, Lunden JJ, Cordes EE. 2016b. Oceanographic patterns and carbonate chemistry in the vicinity of cold-water coral reefs in the Gulf of Mexico: implications for resilience in a changing ocean. *Limnology and Oceanography* **61**:648–665 DOI 10.1002/lno.10242.

Georgian SE, Dupont S, Kurman M, Butler A, Strömberg SM, Larsson AI, Cordes EE. 2016a. Biogeographic variability in the physiological response of the cold-water coral *Lophelia pertusa* to ocean acidification. *Marine Ecology* **37**:1345–1359 DOI 10.1111/maec.12373.

Georgian SE, Shedd W, Cordes EE. 2014. High-resolution ecological niche modelling of the cold-water coral *Lophelia pertusa* in the Gulf of Mexico. *Marine Ecology Progress Series* **506**:145–161 DOI 10.3354/meps10816.

Gruber N, Hauri C, Lachkar Z, Loher D, Frölicher TL, Plattner G-K. 2012. Rapid progression of ocean acidification in the california current system. *Science* **337**:220–223 DOI 10.1126/science.1216773.

Guinotte JM, Orr J, Cairns S, Freiwald A, Morgan L, George R. 2006. Will human-induced changes in seawater chemistry alter the distribution of deep-sea scleractinian corals? *Frontiers in Ecology and the Environment* **4**:141–146 DOI 10.1890/1540-9295(2006)004[0141:WHCISC]2.0.CO2.

Harris KE, DeGrandpre MD, Hales B. 2013. Aragonite saturation state dynamics in a coastal upwelling zone. *Geophysical Research Letters* **40**:2720–2725 DOI 10.1002/grl.50460.

Hauri C, Gruber N, McDonnell AMP, Vogt M. 2013. The intensity, duration, and severity of low aragonite saturation state events on the California continental shelf. *Geophysical Research Letters* **40**:3424–3428 DOI 10.1002/grl.50618.

Hauri C, Gruber N, Plattner G-K, Aline S, Feely R, Hales B, Wheeler PA. 2009. Ocean acidification in the california current system. *Oceanography* **22**:60–71 DOI 10.5670/oceanog.2009.97.

Hennige SJ, Wicks LC, Kamenos NA, Bakker DCE, Findlay HS, Dumousseaud C, Roberts JM. 2014. Short-term metabolic and growth responses of the cold-water coral *Lophelia pertusa* to ocean acidification. *Deep-Sea Research Part II: Topical Studies in Oceanography* **99**:27–35 DOI 10.1016/j.dsr2.2013.07.005.

Hennige SJ, Wicks LC, Kamenos NA, Perna G, Findlay HS, Roberts JM. 2015. Hidden impacts of ocean acidification to live and dead coral framework. *Proceedings of the Royal Society B: Biological Sciences* **282**:20150990 DOI 10.1098/rspb.2015.0990.

Houlbrèque F, Reynaud S, Godinot C, Oberhänsli F, Rodolfo-Metalpa R, Ferrier-Pagès C. 2015. Ocean acidification reduces feeding rates in the scleractinian coral *Styolophora pistillata*. *Limnology and Oceanography* **60**:89–99 DOI 10.1002/lno.10003.

Jansen J, Hill NA, Dunstan PK, McKinlay J, Sumner MD, Post AL, Eléaume MP, Armand LK, Warnock JP, Galton-Fenzi BK, Johnson CR. 2018. Abundance and richness of key Antarctic seafloor fauna correlates with modelled food availability. *Nature Ecology & Evolution* **2**:71–80 DOI 10.1038/s41559-017-0392-3.

Jantzen C, Häussermann V, Försterra G, Laudien J, Ardelan M, Maier S, Ritchter C. 2013. Occurrence of a cold-water coral along natural pH gradients (Patagonia, Chile). *Marine Biology* **160**:2597–2607 DOI 10.1007/s00227-013-2254-0.

Jokiel P, Maragos J, Franzisket L. 1978. Coral growth: buoyant weight technique. In: Stoddart DR, Johannes R, eds. *Coral reefs: research methods.* Paris: UNESCO, 581.

Juranek LW, Feely RA, Peterson WT, Alin SR, Hales B, Lee K, Sabine CL, Peterson J. 2009. A novel method for determination of aragonite saturation state on the continental shelf of central Oregon using multi-parameter relationships with hydrographic data. *Geophysical Research Letters* **36**:4–9 DOI 10.1029/2009GL040778.

Kleypas JA, Buddemeier RW, Archer D, Gattuso J-P, Langdon C, Opdyke BN. 1999. Geochemical consequences of increased atmospheric carbon dioxide on coral reefs. *Science* **284**:118–120 DOI 10.1126/science.284.5411.118.

Kurman MD, Gómez CE, Georgian SE, Lunden JJ, Cordes EE. 2017. Intra-specific variation reveals potential for adaptation to ocean acidification in a cold-water coral from the Gulf of Mexico. *Frontiers in Marine Science* **4**:111 DOI 10.3389/fmars.2017.00111.

Lacharité M, Metaxas A. 2017. Hard substrate in the deep ocean: how sediment features influence epibenthic megafauna on the eastern Canadian margin. *Deep-Sea Research, Part I (Oceanographic Research Papers)* **126**:50–61 DOI 10.1016/j.dsr.2017.05.013.

Langdon C, Atkinson MJ. 2005. Effect of elevated pCO_2 on photosynthesis and calcification of corals and interactions with seasonal change in temperature/ irradiance and nutrient enrichment. *Journal of Geophysical Research: Oceans* **110**:1–16 DOI 10.1029/2004JC002576.

Lee K, Millero FJ, Byrne RH, Feely RA, Wanninkhof R. 2000. The recommended dissociation constants for carbonic acid in seawater. *Geophysical Research Letters* **27**:229–232.

Leuker TJ, Dickson AG, Keeling CD. 2000. Ocean pCO_2 calculated from dissolved inorganic carbon, alkalinity, and equations for K_1 and K_2. Validation based on laboratory measurements of CO_2 in gas and seawater at equilibrium. *Marine Chemistry* **70**:105–119.

Lunden JJ, Georgian SE, Cordes EE. 2013. Aragonite saturation states at cold-water coral reefs structured by *Lophelia pertusa* in the northern Gulf of Mexico. *Limnology and Oceanography* **58(1)**:354–362 DOI 10.4319/lo.2013.58.1.0354.

Lunden JJ, McNicholl CG, Sears CR, Morrison CL, Cordes EE. 2014. Acute survivorship of the deep-sea coral *Lophelia pertusa* from the Gulf of Mexico under acidification, warming, and deoxygenation. *Frontiers in Marine Science* **1**:78 DOI 10.3389/fmars.2014.00078.

Lynn RJ, Simpson JJ. 1987. The California current system: the seasonal variability of its physical characteristics. *Journal of Geophysical Research* **92(C12)**:12947–12966 DOI 10.1029/JC092iC12p12947.

Maier C, Hegeman J, Weinbauer MG, Gattuso J-P. 2009. Calcification of the cold-water coral *Lophelia pertusa* under ambient and reduced pH. *Biogeosciences* **6**:1671–1680.

Maier C, Popp P, Sollfrank N, Weinbauer MG, Wild C, Gattuso J-P. 2016. Effects of elevated pCO_2 and feeding on net calcification and energy budget of the Mediterranean cold-water coral *Madrepora oculata*. *Journal of Experimental Biology* **219**:3208–3217 DOI 10.1242/jeb.127159.

Maier C, Watremez P, Taviani M, Weinbauer MG, Gattuso J-P. 2012. Calcification rates and the effect of ocean acidification on Mediterranean cold-water corals. *Proceedings of the Royal Society B: Biological Sciences* **279**:1716–1723 DOI 10.1098/rspb.2011.1763.

McCulloch M, Trotter J, Montagna P, Falter J, Dunbar R, Freiwald A, Försterra G, Lopez-Correa M, Maier C, Rüggeberg A, Taviani M. 2012. Resilience of cold-water scleractinian corals to ocean acidification: boron isotopic systematics of pH and saturation state up-regulation. *Geochimica et Cosmochimica Acta* **87**:21–34 DOI 10.1016/j.gca.2012.03.027.

Movilla J, Gori A, Calvo E, Orejas C, López-Sanz A, Domínguez-Carrió C, Grinyó J, Pelejero C. 2014. Resistance of two mediterranean cold-water coral species to low-pH conditions. *Water* **6**:59–67 DOI 10.3390/w6010059.

Orejas C, Gori A, Rad-Menéndez C, Last KL, Davies AJ, Beveridge CM, Sadd D, Kiriakoulakis K, Witte U, Roberts JM. 2016. The effect of flow speed and food size on the capture efficiency and feeding behaviour of the cold-water coral *Lophelia pertusa*. *Journal of Experimental Marine Biology and Ecology* **481**:34–40 DOI 10.1016/j.jembe.2016.04.002.

Orr JC, Fabry VJ, Aumont O, Bopp L, Doney SC, Feely RA, Gnanadesikan A, Gruber N, Ishida A, Joos F, Key RK, Lindsay K, Maier-Reimer E, Matear R, Monfray P, Mouchet A, Najjar RG, Plattner G-K, Rodgers KB, Sabine CL, Sarmiento JL, Schlitzer R, Slater RD, Totterdell IJ, Weirig M-F, Yamanaka Y, Yool A. 2005. Anthropogenic ocean acidification over the twenty-first century and its impact on calcifying organisms. *Nature* **437**:681–686 DOI 10.1038/nature04095.

Palacios DM, Bograd SJ, Mendelssohn R, Schwing FB. 2004. Long-term and seasonal trends in stratification in the California Current, 1950–1993. *J Geophys Res C Ocean* **109**:1–12 DOI 10.1029/2004JC002380.

Purser A, Larsson AI, Thomsen L, Van Oevelen D. 2010. The influence of flow velocity and food concentration on *Lophelia pertusa* (Scleractinia) zooplankton capture rates. *Journal of Experimental Marine Biology and Ecology* **395**:55–62 DOI 10.1016/j.jembe.2010.08.013.

Robbins LL, Hansen ME, Kleypas JA, Meylan SC. 2010. CO2calc: a user-friendly seawater carbon calculator for Windows, Mac OS X and iOS (iPhone). US Geol Surv Open-File Rep 2010-1280 17.

Raybaud V, Tambutté S, Ferrier-Pàges C, Reynaud S, Venn AA, Tambutté E, Nival P, Allemand D. 2017. Computing the carbonate chemistry of the coral calcifying medium and its response to ocean acidification. *Journal of Theoretical Biology* **424**:26–36.

Roberts JM, Wheeler AJ, Freiwald A, Cairns SD. 2009. *Cold-water corals: the biology and geology of deep-sea coral habitats.* Cambridge: Cambridge University Press.

Rykaczewski RR, Dunne JP. 2010. Enhanced nutrient supply to the California Current Ecosystem with global warming and increased stratification in an earth system model. *Geophysical Research Letters* **37**:1–5 DOI 10.1029/2010GL045019.

Siegenthaler U, Stocker TF, Monnin E, Lüthi D, Schwander J, Stauffer B, Raynaud D, Barnola J-M, Fischer H, Masson-Delmotte V, Jouzel J. 2005. Stable carbon cycle-climate relationship during the Late Pleistocene. *Science* **310**:1313–1317 DOI 10.1126/science.1120130.

Thresher RE, Tilbrook B, Fallon S, Wilson NC, Adkins J. 2011. Effects of chronic low carbonate saturation levels on the distribution, growth and skeletal chemistry of deep-sea corals and other seamount megabenthos. *Marine Ecology Progress Series* **442**:87–96 DOI 10.3354/meps09400.

Underwood AJ. 1997. *Experiments in ecology: their logical design and interpretation using analysis of variance.* Cambridge: Cambridge University Press.

Wang D, Gouhier TC, Menge BA, Ganguly AR. 2015. Intensification and spatial homogenization of coastal upwelling under climate change. *Nature* **518**:390–394 DOI 10.1038/nature14235.

Wickes L. 2014. The effect of acidified water on the cold-water coral, *Lophelia pertusa*: distribution in the Southern California Bight and analysis of skeletal dissolution. Master of Science thesis, College of Charleston, 89 p.